

Impact Damage on Brittle Materials with Small Spheres (I)

Su Chang Woo¹, Moon Saeng Kim², Hyung Seop Shin³, Hyeon Chul Lee⁴

¹ Department of Mechanical Design Engineering, Graduate School, Pusan National University, Pusan, South Korea

² School of Mechanical Engineering, Pusan National University, Pusan, South Korea

³ School of Mechanical Engineering, Andong National University, Andong, Kyungbuk, South Korea

⁴ Department of Computer Aided Design, Doowon Technical College, Ansong, Kyunggi, South Korea

ABSTRACT

Brittle materials such as glasses and ceramics, which are very weak under impact loading, show fragile failure mode due to their low fracture toughness and crack sensitivity. When brittle materials are subjected to impact by small spheres, high contact pressure occurs at the impacted surface causing local damage on the specimen. This damage is a dangerous factor in causing the final fracture of structures. In this research, the crack propagation process of soda-lime glass by the impact of small spheres is explained and the effects of several constraint conditions for impact damage were studied by using soda-lime glass; that is, the effects for the materials and sizes of impact ball, thickness of specimen and residual strength were evaluated. Especially, this research has focused on the damage behavior of ring cracks, cone cracks and several other kinds of cracks.

Keywords : Impact damage, Ring crack, Cone crack, Crushing, Erosion, Radial crack, Lateral crack, Splinter crack

1. Introduction

Metals, ceramics and plastics generally classify most part of industrial materials. Ceramics are brittle materials, which have high specific stiffness, thermal and wear resistance. Ceramic materials are used in structural members such as automobiles, aircraft engines and rotors or blades of gas turbines that are exposed to severe environments of high temperature and corrosion. However brittle materials are weak under impact loading because these materials have characteristics such as low fracture toughness and crack sensitivity, which are easily fractured by small defects and cracks. When brittle materials are subjected to impact by solid particles, high contact pressure occurs at the impacted surface causing local damage on the specimen since there are little plastic deformations due to contact pressure in contrast to metallic materials. This local damage is a dangerous factor in causing final fracture of structures.

In order to examine closely the mechanism of surface damage of ceramics and the phenomenon of strength decline due to damage occurrence, many studies⁽¹⁻⁸⁾ have been performed on the basis of Hertzian contact theory by modeling solid particles on small spheres. But there are no detailed presentations to explain how boundary conditions of brittle materials have an influence on impact damage. In this research, by using soda-lime glass, which is one of the most brittle materials, the effects of the material, size, and velocity of impact particles and the thickness of the specimen were investigated.

2. Experiment

2.1 Impact Experiment

An impact experiment is carried out using the principle of air gun by a compressor as shown in Fig. 1.

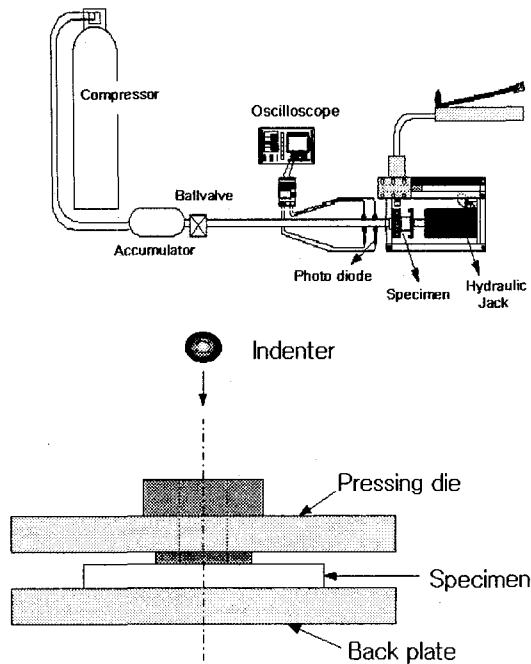


Fig. 1 schematic diagram of whole experimental system and specimen combined with pressing die

The operation process is as follows. A carrier containing a ball is installed inside a gun barrel. The ball valve is opened momentarily by controlling the air pressure with a compressor. Just then the carrier is accelerated by the compressed air and is stopped by a stopper, which is located 40mm ahead of the specimen. The specimen is subjected to impact by a steel ball flying continuously due to inertia. The impact velocity of the steel ball is controlled by the compressed air. The impact velocity of the steel ball was measured by a couple of diodes connected to an oscilloscope. The velocity of the steel ball was measured to an accuracy of 3% by timing its flight between two diodes situated close to the end of the barrel of the air gun. Two photo diodes are installed in

position of 100mm and 200mm in front of the specimen.

2.2 Specimen

The dimensions of the soda-lime glass specimen are of length 400mm, width 40mm, and thickness 5mm. Steel balls of 2mm, 3mm and 4mm in diameter and a zirconia ball of 3mm in diameter were used for the test. The mechanical properties of the specimen and indenters are shown in Table 1.

Table 1 Mechanical properties of the specimen and indenters

Material	ρ (g/cm ³)	E (GPa)	ν	H _v (Gpa)	C ₀ (m/s)
Glass	2.5	75	0.25	6.5	5477
Steel ball	7.85	210	0.29	8.0	•
Zirconia ball	6	300	0.14	10	•

3. Results and Discussion

3.1 Crack propagation process of soda-lime glass

Fig. 2 shows the schematic crack propagation process according to the impact velocity of the 3mm steel ball. Ring crack occurs at $v=9\text{m/s}$ and cone crack ($v=10.3\text{m/s}$) begins to appear at the edge of the initial ring crack. As the velocity of the steel ball is increased, the ring crack grows continuously in the radial direction, and the cone crack grows in the direction of thickness. Lateral crack ($v=24.9\text{m/s}$) grows in the inclined surface of cone crack, and radial crack ($v=29.5\text{m/s}$) begins to grow from the outermost ring crack. As the velocity of the impact particles increases continuously, the phenomenon of crushing and erosion on the specimen occurs causing the cone crack to separate from the specimen. Finally the specimen is fractured at $v=47.6\text{m/s}$.

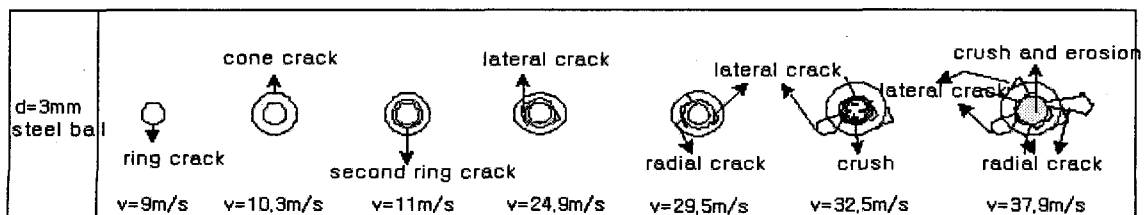


Fig. 2 Crack propagation process by impact of small sphere

The major cause of fracture comes from radial cracks, which grow in the radial direction. Sometimes the fracture comes in combinations of radial cracks and lateral cracks, which occur at the inclined surface of the cone crack and grow toward the surface of the specimen.

3.2 Effects for the material of impact particles

3.2.1 Variation of ring crack

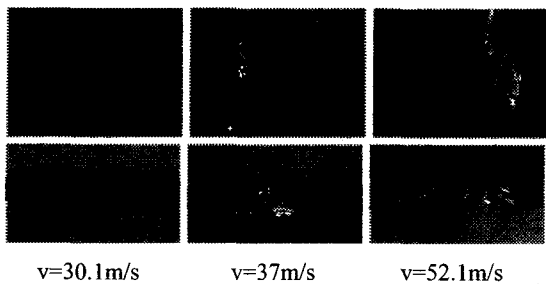


Fig. 3 Behavior of specimen by impact of steel ball

In order to observe the effects of the impact particle's material, the experiment is carried out using the 3mm in diameter steel and the zirconia ball. Fig. 3 shows photographs of the front and side view of the impact damage on the specimen by the steel ball. Fig. 4 shows the size variation of ring crack according to the material and the velocity of the impact particles.

Looking over the photos in Fig. 3, in the case of $v=30.1\text{m/s}$, ring crack and cone crack appear simultaneously and it is difficult to distinguish the cone crack from the photograph. In the case of $v=37\text{m/s}$ it is observed that the lateral crack appears from the inclined surface of the cone crack. At the velocity of 52.1m/s , the growing of radial and lateral cracks, crushing, and the phenomenon of erosion are observed. The cone crack is perfectly separated from the specimen as shown in photographs. Observing the propagation of ring crack, the innermost ring crack (d_i) increases slowly in proportion to the impact velocity of the steel ball without regard to the material. On the other hand, the outermost ring crack (d_o) appears larger in the case of the steel ball than the zirconia ball above the velocity of 30m/s . This fact results from the difference of momentum; the density of the steel ball ($\rho=7.85$) is larger than that of the zirconia ball ($\rho=6.0$). In the cases of ring crack, when the impact particle comes in contact with the specimen, the radial stress is compressive under the contact surface, but

is tensile in the outside of the contact surface. Therefore, the maximum shear stress occurs in the vicinity of the boundary, and causes ring crack.⁽⁹⁾

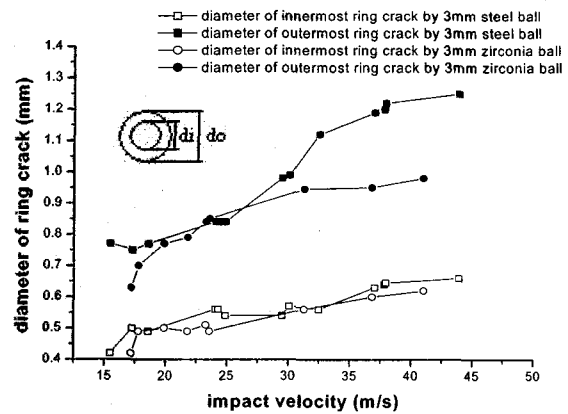


Fig. 4 Diameter of ring crack by steel ball and zirconia ball

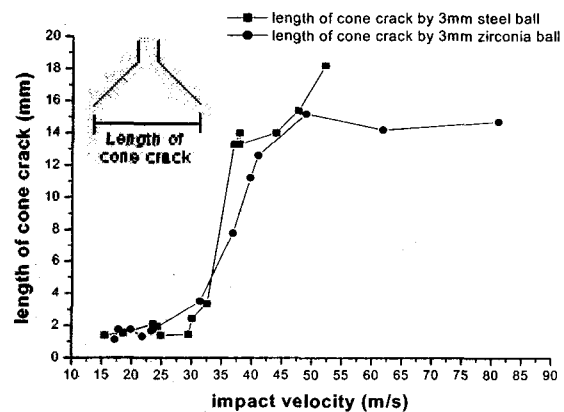


Fig. 5 Length of cone crack by steel ball and zirconia ball

3.2.2 Variation of Cone Crack

Fig. 5 shows the variation of cone crack, which appears after ring crack. The propagation of cone crack occurs along the progressive direction of the stress wave, which is developed in the low part of the contact surface and occurs from the innermost ring crack.

Observing the variation of cone crack according to the material of the impact particles in Fig. 5, the length of cone crack is consistent up to $v=30\text{m/s}$ in both cases of the steel and zirconia balls, thereafter increasing rapidly. After $v=30\text{m/s}$, the length of cone crack by the steel ball increases up to $v=50\text{m/s}$ resulting in fracture. The length of cone crack by the zirconia ball does not increase after $v=50\text{m/s}$ but keeps steady with increasing

velocity. Following the ring and cone crack, crushing occurs in the specimen as the impact velocity continues to increase. Crushing occurs at $v=32.5\text{m/s}$ in the case of the steel ball and at $v=48.9\text{m/s}$ in the case of the zirconia ball. After the appearance of crushing, the lateral crack and the ring crack grow largely. It is considered that the strain energy accumulated in the region of plastic deformation provides the driving force for the lateral crack and the radial crack.

In the case of the steel ball, the cone crack is separated from the specimen at $v=47.6\text{m/s}$, thereafter the specimen is fractured perfectly. In the case of the zirconia ball, which has little relative momentum, the cone crack is separated at $v=49\text{m/s}$ (see Fig. 6) and the specimen is fractured at $v=67.1\text{m/s}$. Such a fracture of the specimen occurs from the growth of the radial crack due to the increase in velocity. Sometimes the combination of lateral crack and radial crack causes large damage and fracture of the specimen.⁽¹⁰⁾ Also, the lateral crack grows rapidly when the turn-up phenomenon occurs in the edge of the inclined surface of cone crack. Fig. 7 shows that the lateral crack occurred to the inclined surface of the cone crack which combines with the turn-up region and grows rapidly. Table 2 shows the critical velocities of crack appearance according to the material of the impact particles.



Fig. 6 Cone crack Separated from Specimen ($v=49\text{m/s}$, zirconia ball)



Fig. 7 Turn-up phenomenon and development of lateral crack ($v=42\text{m/s}$, zirconia ball)

Table 2 Critical velocities for the impact ball materials

materials	ring crack (m/s)	crushing (m/s)	cone crack separation (m/s)	fracture (m/s)
steel	9	32.5	47.6	50
zirconia	11.5	39.7	49	67.1

3.3 Effects for the size of impact particles

In order to investigate the effects of the size

(diameter) of the impact particles, the impact experiments are carried out using steel balls of 2, 3, and 4mm in diameter. The diameter variation of ring cracks according to the size of impact particles is shown in Fig. 8. The graph shows that the size of the outermost and the innermost ring crack is in proportion to the size of the impact particle and grows gradually with increasing velocity. As the size of the impact particle becomes larger, the slopes of the data of the outermost and the innermost ring crack also increases. Especially in the case of the 4mm-diameter steel ball, the length of the outermost (do) and the innermost (di) ring crack grows rapidly after $v=19.6\text{m/s}$. The larger the size of the steel ball, the shorter the velocity range of data. This is because crushing occurs at a low velocity when the size of the impact particles becomes large.

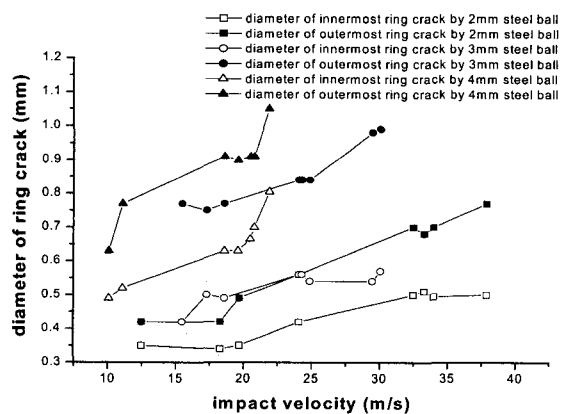


Fig. 8 Diameter of ring crack by the size of steel ball

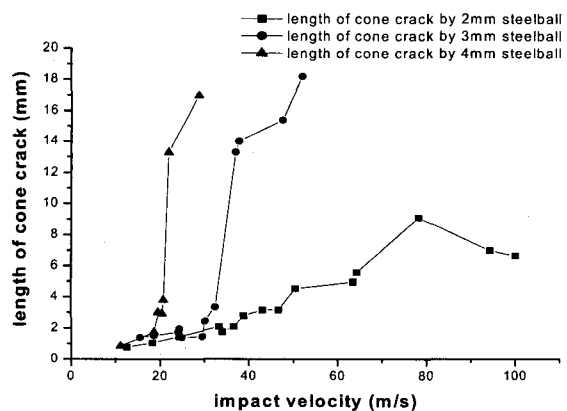


Fig. 9 Length of cone crack by the size of steel ball

Fig. 9 shows the length variation of cone crack in

relation to the size of the impact particles. In the case of the 2mm-diameter steel ball, the length of cone crack grows up to 78.1m/s gradually but thereafter decreases and does not grow in the direction of depth. It is thought that a small steel ball by itself would plastically deform at high velocity and absorb impact energy. At the velocity of 60m/s, the plastic deformation of the steel ball was observed. In the case of the 3mm and 4mm-diameter steel balls, the length of cone crack grows rapidly above the specific velocity. And in the case of the 2mm-diameter steel ball, the separation and fracture of cone cracks do not occur till the velocity of 110m/s. But as shown in Fig. 10, the splinter cracks appear at the velocity range of 75.2m/s~100m/s. Those splinter cracks appear easily when the mass of the impact particle is small relative to the thickness of the specimen (5mm-thick specimen, 2mm-diameter steel ball). Table 3 shows the critical velocities of cracks for different steel ball sizes.

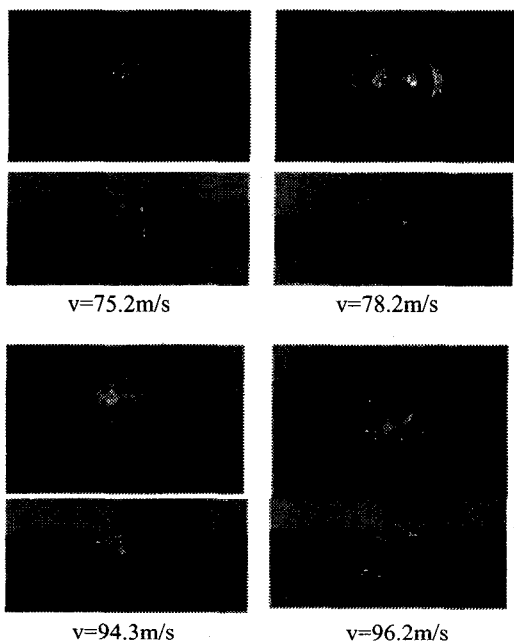


Fig. 10 Appearance of splinter cracks by impact of steel

3.4 Effects for the thickness of specimen

Effects of the thickness of the specimen are examined using the 5mm and 8mm-thick specimen. Fig. 11 shows the behavior of ring crack for the thickness of specimen. The graph shows that at the same velocity the diameters of the innermost and outermost ring cracks in

Table 3 Critical velocities for the size of steel ball

ball size	Ring crack (m/s)	crushing (m/s)	cone crack separation (m/s)	Fracture (m/s)
2mm	12.5	43.1	×	×
3mm	9	32.5	47.6	50
4mm	7.8	21	21.9	28.7

the 5mm-thick specimen are larger than those in the 8mm-thick specimen. The variation of the innermost and outermost ring cracks in the 5mm and 8mm-thick specimens show similar behavior with increasing velocity.

On the other hand, as shown in Fig. 12, in the case of the 5mm-thick specimen, the length of the cone cracks grow rapidly above the velocity of 30m/s, and in the case of the 8mm-thick specimen the length of the cone cracks increase gradually with increasing velocity. This result shows that the formation of the cone crack is delayed on account of the appearance of splinter cracks between the velocities of 36.8m/s and 100m/s in the 8mm-thick specimen. This is the same result shown in the 5mm-thick specimen. And in the case of the 5mm-thick specimen the cone crack is perfectly separated from the specimen at the velocity of 47.6m/s, but in the case of the 8mm-thick specimen the cone crack is not separated from the specimen until the velocity comes to 100m/s. In the case of the 5mm-thick specimen, crushing occurs at $v=32.5m/s$, and at $v=34.7m/s$ in the case of the 8mm-thick specimen. After the appearance of crushing, the growth of the cone crack becomes dull and does not grow in the direction of depth.

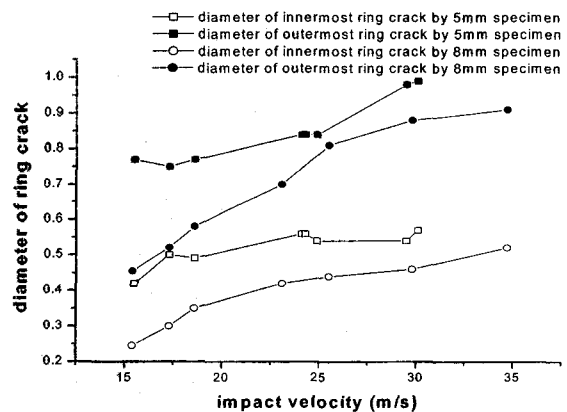


Fig. 11 Diameter of ring crack by steel ball for the thickness of specimen

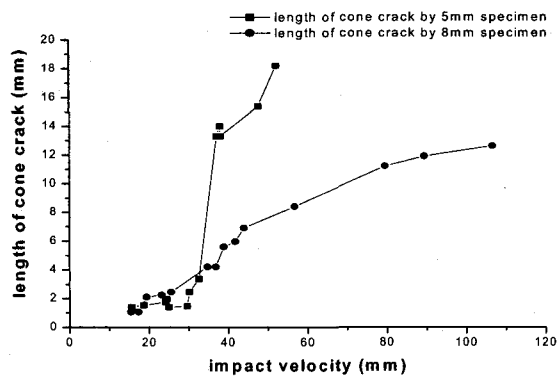


Fig. 12 Length of cone crack by steel ball for the thickness of specimen

3.5 Evaluation of residual strength

In order to evaluate residual strength for the impacted specimen, a 4-point bending test was carried out as shown in Fig. 13. Fig. 14 shows the variation of residual strength according to the material of impact particles. After the specimen is impacted by the impact particle, the residual strength of the specimen has the values of 70~80MPa within $v=32.5\text{m/s}$ without regard to the material. The dispersion of such values means that ring cracks or initial cone cracks never have an effect on the residual strength because the width of the specimen(40mm) is much larger than the size of the ring cracks or initial cone cracks. It is observed that the failure surface by the 4-point bending test does not pass through ring cracks or cone cracks in the specimen. Therefore in the case of low velocity impact the residual strength is influenced by the surface roughness or the defects on the surface of the specimen rather than the damage parts by the impact of particles. After $v=37\text{m/s}$ and $v=31.3\text{m/s}$, in the cases of the steel and zirconia ball, respectively, it is observed that the residual strength decreases abruptly due to the rapid growth of cone cracks.

Fig. 15 shows the effects of the residual strength for the size of impact particles. The residual strength decreases rapidly at the velocities where the length of cone crack is greater than 4mm, that is, at $v=50.5\text{m/s}$ in the 2mm steel ball, $v=37\text{m/s}$ in the 3mm steel ball, and 21.9m/s in the 4mm steel ball. Therefore, when the length of the cone crack is greater than 4mm the bending strength is influenced greatly regardless of the size of the impact particles. The depth of the cone crack effects the residual strength greater than the length of the cone crack

in the pure bending test.

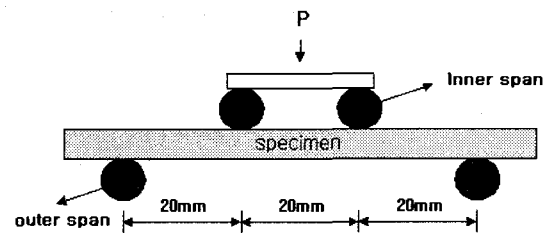


Fig. 13 Scheme of 4-point bending test

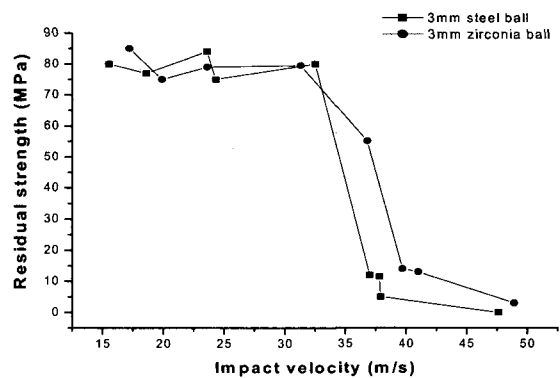


Fig. 14 Residual strength for the impact ball material

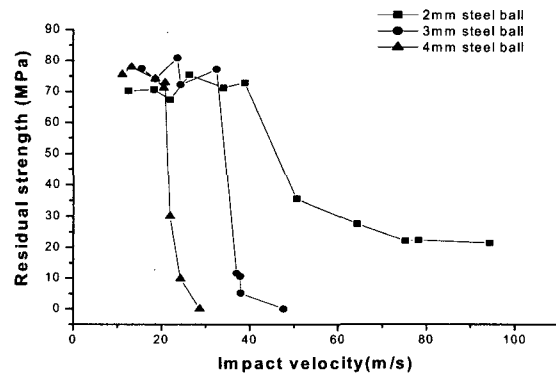


Fig. 15 Residual strength for the size of steel ball

4. Conclusions

Effects of the impact damage of soda-lime glass were evaluated through the crack propagation process, the impact particles, the impact materials, and the residual strength of the specimen.

1. The crack propagation process for the impact-loaded soda-lime glass was understood.

2. The material of impact particles has no effect on the variation of the innermost ring crack, but variation of the outermost ring crack is affected by the materials which have high density. And the length of cone crack increases rapidly above a special velocity without regard to the material of impact particles.
3. The length of the outermost and the innermost ring crack is in proportion to the size of the impact particles and grows gradually according to the velocity. And as the size of impact particles is larger, the size of the outermost ring crack increases rapidly.
4. When the mass of the impact particle is small compared to the thickness of the specimen, the splinter crack appears and grows, consequently the growth of the cone crack is delayed.
5. The ring crack and the initial cone crack have no influence on the residual strength. But when the length of cone crack becomes above 4mm the bending strength is influenced seriously regardless of the size of impact particles. The depth of cone crack rather than the length of cone crack has influence on the residual strength.
6. "Impact of Small Steel Spheres on Glass Surfaces," *J. Mater. Sci.*, Vol. 12, pp. 1573~1586, 1977.
6. Tillet. J.R.A., "Fracture of Glass by Spherical indenters," *Proc. Roy. Soc.*, Vol. B69, pp. 47~54, 1956.
7. Fields. J.E., Sun. Q. and Townsend. D., "Ballistic Impact of Ceramics," *Inst. Phy. Conf. Series No. 102*, pp. 387~393, 1989.
8. Persion, J., Breder, K. and Rowcliffe, D.J., "Loading Rate Effects During Indentation and Impact on Glass with Small Spheres," *J. Mater. Sci.*, Vol. 28, pp. 6484~6489, 1993.
9. Chaudhri, M.M. and Walley, S.M., "Damage to Glass Surfaces by the Impact of small Glass and Steel Sphere," *Philos. Mag., Part A*, Vol. 37, No. 2, pp. 153~165, 1978.
10. Suh, C.M, Shin, H.S, Chung, S.M., and Hwang, B.W. "An Experimental Study on Damage Mechanism of Glass Resulting from Partical Impact," *Trans KSME(A)*, Vol. 20, No. 6, pp. 1903~1912, 1996.

Acknowledgement

This work was supported by Grant No. 2000-1-30400-015-2 from the Basic Research Program of the KOSEF (Korea Science and Engineering Foundation).

References

1. S. Timoshenko and J. N. Gooder., "Theory of Elasticity," McGraw-Hill Book Co., New york, pp. 383, 1965.
2. Frankm F. C. and Lawn, B.R., "On the Theory of Hertzian Fracture," *Proc. R. Soc.*, Vol. A209, pp. 291~306, 1967.
3. Johnson, K. L., "Contact Mechanics," Cambridge University Press, New York, 1985.
4. Tsai, T.M., "Dynamic Contact Stresses produced by the impact of an Axisymmetrical Projectile on an Elastic Half-Space," *Int. J. Solid Struct.*, Vol. 7, pp. 543~558, 1971.
5. Knight, C.G., Swain, M. V. and Chaudhri, M. M.,